Am J Physiol Lung Cell Mol Physiol 299: L905–L914, 2010.
First published October 1, 2010; doi:10.1152/ajplung.00094.2010.

A tandem repeat of a fragment of *Listeria monocytogenes* internalin B protein induces cell survival and proliferation

Ognoon Mungunsukh,[1]* Young H. Lee,[1]* Ana P. Marquez,[1] Fabiola Cecchi,[2] Donald P. Bottaro,[2] and Regina M. Day[1]

[1]*Department of Pharmacology, Uniformed Services University of the Health Sciences and* [2]*Urologic Oncology Branch, Center for Cancer Research, National Cancer Institute, Bethesda, Maryland*

Submitted 24 March 2010; accepted in final form 1 October 2010

Mungunsukh O, Lee YH, Marquez AP, Cecchi F, Bottaro DP, Day RM. A tandem repeat of a fragment of *Listeria monocytogenes* internalin B protein induces cell survival and proliferation. *Am J Physiol Lung Cell Mol Physiol* 299: L905–L914, 2010. First published October 1, 2010; doi:10.1152/ajplung.00094.2010.—Hepatocyte growth factor (HGF) is critical for tissue homeostasis and repair in many organs including the lung, heart, kidney, liver, nervous system, and skin. HGF is a heterodimeric protein containing 20 disulfide bonds distributed among an amino-terminal hairpin, four kringle domains, and a serine protease-like domain. Due to its complex structure, recombinant production of HGF in prokaryotes requires denaturation and refolding, processes that are impractical for large-scale manufacture. Thus, pharmaceutical quantities of HGF are not available despite its potential applications. A fragment of the *Listeria monocytogenes* internalin B protein from amino acids 36–321 ($InlB_{36–321}$) was demonstrated to bind to and partially activate the HGF receptor Met. $InlB_{36–321}$ has a stable β-sheet structure and is easily produced in its native conformation by *Escherichia coli*. We cloned $InlB_{36–321}$ ($1\times InlB_{36–321}$) and engineered a head-to-tail repeat of $InlB_{36–321}$ with a linker peptide ($2\times InlB_{36–321}$); $1\times InlB_{36–321}$ and $2\times InlB_{36–321}$ were purified from *E. coli*. Both $1\times$ and $2\times InlB_{36–321}$ activated the Met tyrosine kinase. We subsequently compared signal transduction of the two proteins in primary lung endothelial cells. $2\times InlB_{36–321}$ activated ERK1/2, STAT3, and phosphatidylinositol 3-kinase/Akt pathways, whereas $1\times InlB_{36–321}$ activated only STAT3 and ERK1/2. The $2\times InlB_{36–321}$ promoted improved motility compared with $1\times InlB_{36–321}$ and additionally stimulated proliferation equivalent to full-length HGF. Both the $1\times$ and $2\times InlB_{36–321}$ prevented apoptosis by the profibrotic peptide angiotensin II in cell culture and ex vivo lung slice cultures. The ease of large-scale production and capacity of $2\times InlB_{36–321}$ to mimic HGF make it a potential candidate as a pharmaceutical agent for tissue repair.

apoptosis; angiotensin II; Akt; ERK1/2

HEPATOCYTE GROWTH FACTOR (HGF) is pleiotropic, inducing proliferation, motility, and morphogenesis in a cell type-specific manner (53). The genes encoding HGF and its receptor Met are required for embryogenesis (4), and knockout mice for *HGF* or *MET* die in utero from defects in development of the liver and placenta (52). In the adult, HGF is involved in tissue homeostasis, especially for cell survival and maintenance of epithelial and endothelial cells in a variety of tissues (40). *HGF* gene expression and the release of HGF protein from the extracellular matrix are also induced by tissue injury, and HGF plays a key role in normal tissue repair in many organs (22, 29, 31, 37, 40, 49, 51, 54, 64). In animal models, HGF given either exogenously as a protein or via gene therapy has been demonstrated to promote normal tissue repair and prevent fibrotic remodeling and scarring (20, 27, 41, 46, 57, 61, 62).

HGF signaling through its receptor Met is considered an important factor for epithelial repair following lung injury (10). Defects in HGF signaling have been observed in patients with IPF and in patients with systemic sclerosis, who are susceptible to lung fibrosis (5, 23, 39). Abnormally low levels of HGF have been correlated with increased severity of pulmonary diseases in preterm infants (33). HGF treatment has been shown to mitigate lung injury and induce normal tissue repair in a variety of experimental animal models including: *1*) fibrotic remodeling in response to bleomycin (66); *2*) allergic airway inflammation in response to ovalbumin (50); *3*) acute lung injury induced by intratracheal infusion of HCl (49); *4*) acute respiratory distress syndrome following treatment with LPS (25); and *5*) elastase-induced emphysema (56). The efficacy of HGF in mitigating such a wide variety of lung injuries illustrates the overall importance of HGF in normal alveolar repair processes.

HGF is synthesized in cells as a 90-kDa polypeptide chain containing an amino-terminal hairpin, four kringle domains, and a serine protease-like domain. Functionally active HGF protein requires correct folding in a conformation that contains 20 disulfide bonds (53). HGF binding to its receptor Met, a tyrosine kinase receptor with a single transmembrane domain, results in activation of multiple downstream signaling pathways, most notably the p42/p44 MAPK (ERK1/2), STAT3, and PI3K/Akt pathways. We and others have demonstrated that the combination of these signaling events are required for motility, anti-apoptotic activity, and proliferation in cell culture (12).

Despite the obvious potential therapeutic uses of HGF, the complexity of the full-length HGF protein structure has severely hindered its development as a pharmaceutical agent. Attempts have been made to use smaller fragments of the HGF molecule, such as NK1 or NK2, that are naturally occurring isoforms of HGF containing only the amino-terminal hairpin and the first kringle or first and second kringle domains, respectively (8). Although NK1 can induce motility, survival, and proliferation, its potency is lower than that of full-length HGF (8). NK2 activation of Met results in cell motility in transformed cells, but not cell survival or proliferation (12). But most importantly, despite their smaller size, large-scale production of biologically active NK1 and NK2 has not yet succeeded, as their synthesis in bacteria still requires time-consuming and expensive steps of refolding and renaturation to attain correct conformation (58).

Other proteins, such as the internalin B (InlB) protein produced by *Listeria monocytogenes*, have been identified that

* O. Mungunsukh and Y. H. Lee contributed equally to this work.

Address for reprint requests and other correspondence: R. M. Day, Dept. of Pharmacology, Bldg. C, Rm 2023, 4301 Jones Bridge Rd., Bethesda, MD 20814-4799 (e-mail: rday@usuhs.mil).

bind to Met. The process of *L. monocytogenes* invasion of a host cell involves a "zipper" mechanism, in which the bacterium attaches to the host cell membrane and triggers a series of intracellular signaling cascades (63). The InlB protein of *L. monocytogenes* is one of two proteins found to participate in binding of the bacterium to the host cell. Full-length InlB was found to partially activate the Met receptor, resulting in ERK1/2 pathway activation (63). In some cells, full-length InlB was also shown to activate the phosphatidylinositol 3-kinase (PI3K)/Akt pathway (3, 6). Met binding and signal transduction by InlB correlated with increased invasiveness of the pathogen (2, 24, 63). The structure of the internalin domain of InlB (amino acids 36–321) was analyzed by crystallography in complex with a portion of the extracellular region of the Met receptor (the semaphorin, the cysteine-rich, and first two Ig-like domains; amino acids 25–741) (48). Structural analysis revealed that the primary affinity-determining contacts occur between the concave face of the $InlB_{36–321}$ leucine-rich repeat (LLR) region and the Ig1 domain of Met. The $InlB_{36–321}$ fragment makes secondary contacts through its interrepeat (IR) region with the semaphorin domain of Met, and binding in this region is thought to be required for receptor activation (48). Unlike full-length InlB or full-length HGF, the $InlB_{36–321}$ fragment failed to induce DNA synthesis in MDCK cells (48). While the work described here was in progress, a stable dimer of $InlB_{36–321}$ was produced by engineering disulfide bonds centered on the convex face of the LRR helix, allowing the formation of an anti-parallel arrangement of two $InlB_{36–321}$ fragments (15). The crystal structure was solved with the Met fragment demonstrating that a symmetrical dimer of $InlB_{36–321}$ assembled having a stoichiometry of 2:2 with the $Met_{25–741}$ ectodomain. Furthermore, the $InlB_{36–321}$ dimer induced motility and proliferation in MDCK cells.

Here we show that the $InlB_{36–321}$ fragment of *L. monocytogenes* ($1\times InlB_{36–321}$) induces activation of ERK1/2 and STAT3 in primary lung endothelial cells and has anti-apoptotic and motogenic activity. We constructed an expression vector encoding a head-to-tail repeat of $InlB_{36–321}$ ($2\times InlB_{36–321}$) with a short peptide linker. We demonstrate that the resulting tandem dimer $2\times InlB_{36–321}$ induces signaling through ERK1/2, PI3K/Akt, and STAT3 pathways, and has improved migratory activity compared with the $1\times InlB_{36–321}$. The $2\times InlB_{36–321}$ also induces proliferation in primary lung cells equivalent to full-length HGF. We report for the first time these activities of InlB associated with mitogenesis, cell survival, and motogenesis in primary cells.

MATERIALS AND METHODS

Reagents. Genomic DNA from *L. monocytogenes* was the generous gift of Dr. Laurel Lenz (National Jewish Medical and Research Center, Univ. of Colorado, Denver). Phospho-ERK1/2 antibody was purchased from Signal Transduction Laboratories (Beverly MA); anti-ERK1/2 was from Upstate Biotech (Charlottesville, VA); phospho-Akt, total Akt, phospho-STAT3, total STAT3, active caspase 3, and uncleaved caspase 3 antibodies were purchased from Cell Signaling Technology (Danvers, MA). The primary anti-phosphotyrosine antibody 4G10 was purchased from Millipore (Billerica, MA). Angiotensin II (Ang II) peptide was purchased from Bachem (Torrance, CA). The primary antibody α-tubulin was purchased from Sigma (St. Louis, MO). β-actin antibody was from Santa Cruz Biotechnology (Santa Cruz, CA).

Cloning and expression of the L. monocytogenes $InlB_{36–321}$. The InlB sequence from amino acid 36–321 (GenBank acc. no. DQ132796, nucleotide sequence from 106 to 963) was amplified using the *Pfu* DNA polymerase (Stratagene, La Jolla, CA), *L. monocytogenes* genomic DNA, and the primers: forward 5′-ggg aa**c acg tg**G AGA CTA TCA CCG TGT CAA C-3′ and reverse 5′-cg**g gat cct** att aCT CTT TCA GTG GTT GGG TTA CT-3′, with uppercase bases corresponding to *InlB* gene sequences and lowercase bases indicating 5′-extensions with restriction enzyme sites (bold) for *Pml*I and *Bam*HI, respectively. The monomeric InlB fragment is designated as $1\times InlB_{36–321}$. A tandem repeat was constructed of the $InlB_{36–321}$ fragment ($2\times InlB_{36–321}$) by joining the two *Acl*I cut PCR products, which were amplified using the forward or reverse primers described previously and a second reverse primer 5′-ttt gga tcc **aac gtt** CTC TTT CAG TGG TTG GGT TAC TTC-3′ or a second forward primer 5′-ttt gga tcc **aac gtt** CTC TTT CAG TGG TTG GGT TAC TTC-3′, respectively, both containing the *Acl*I site (bold). PCR condition was as follows: an initial denaturation of 94°C for 3 min; 10 cycles of 94°C for 30 s, 55°C for 30 s, and 72°C for 2.5 min; 25 cycles of 94°C for 30 s, 55°C for 30 s, and 72°C for 2 min; with a final extension of 5 min at 72°C. The PCR products were cloned into the pET302/NT-His vector (Invitrogen, Carlsbad, CA) using the *Pml*I and *Bam*HI sites, and insertions were verified by DNA sequencing.

The NH_2-terminal 6× His-tagged recombinant $1\times InlB_{36–321}$ and $2\times InlB_{36–321}$ were introduced into *E. coli* BL21-CodonPlus cells according to the manufacturer's protocol (Stratagene, La Jolla, CA). Protein expression was induced at bacterial cell growth of OD_{600} = 0.6–0.8 with 1 mM isopropyl β-D-1-thiogalactopyranoside for 3 h at 37°C. Bacterial cells were collected by 10 min of centrifugation at 4,000 *g*, washed with lysis buffer (50 mM NaH_2PO_4, 300 mM NaCl, 10 mM imidazole, pH 8.0), and stored overnight at −20°C. The next day, cells were resuspended in lysis buffer (0.3 g/ml); 1 mg/ml lysozyme (Novagen, Madison, WI) was added and incubated for 30 min on ice. Benzonase (1 U/ml; Novagen) was added and incubated for an additional 15 min, and then cells were disrupted for 5 × 10 s using an ultrasonicator at 50% output control (Heat Systems-Ultrasonics, Plainview, NY). Cell debris was removed by centrifugation (30 min, 47,000 *g*); cleared cell lysates were used for protein purification.

Protein purification. The 6× His-tagged $1\times InlB_{36–321}$ and $2\times InlB_{36–321}$ were purified using Ni-NTA Superflow according to the QIAexpressionist protocol (Qiagen, Valencia, CA). Briefly, CellThru 10-ml disposable columns (Clontech Laboratories, Mountain View, CA) were packed by gravity flow with 50% Ni-NTA Superflow (Qiagen, 2.5 ml/column). After equilibration using 20 ml of lysis buffer, the column was loaded with cell lysate and washed with 10 ml of lysis buffer containing 20 and 60 mM imidazole. Proteins were eluted from the column using 10 ml of lysis buffer containing 250 mM imidazole. Fractions from each purification step were analyzed by 10% SDS-PAGE. After identification of fractions containing the InlB protein, the imidazole-eluate was diluted to 1:10 with running buffer (5 mM phosphate buffer, pH 6.8) and loaded to hydroxyapatite column (Bioscale Mini CHT Ceramic Hydroxyapatite Cartridges, 5 ml; BioRad, Hercules, CA) equilibrated with 30 ml of running buffer. The column was washed once with 25 ml of running buffer and subsequently with 25 ml of running buffer containing 1 M NaCl. Proteins were eluted using a linear gradient of phosphate buffer (10 mM, pH 6.0, and 500 mM, pH 7.0; 25 ml each). Fractions from each purification step were analyzed by 10% SDS-PAGE. Amicon Ultra-15 filter units (10 kDa; Millipore) were used according to the manufacturer's instructions to concentrate the purified protein, to remove imidazole, and to reduce salt concentration. Endotoxin was removed from the purified and concentrated protein solution using the Detoxi-Gel Endotoxin Removal Gel according to the manufacturer's protocol (Pierce Biotechnology, Rockford, IL).

Cell culture. Bovine pulmonary artery endothelial cells (PAEC) were purchased from Cell Applications (San Diego, CA). *Passages*

2–8 cells were used for all experiments and were cultured in RPMI 1640 (Invitrogen) supplemented with 10% FBS (Gemini, Woodland, CA), 1% penicillin/streptomycin, and 0.5% fungizone (Invitrogen). Cells were grown in 5% CO_2 at 37°C in a humidified atmosphere in a cell culture incubator. 184B5 mammary epithelial cells were grown as previously described (12). Cells were grown in RPMI 1640 medium (Invitrogen) with 10% FBS (Gemini Bioproducts) with 5 ng/ml epidermal growth factor (BD Biosciences Pharmingen, San Diego, CA) and 1% penicillin/streptomycin. EA.hy926 cells, a human umbilical vein cell line, were purchased from American Type Culture Collection (Manassas, VA) and cultured according to the manufacturer's instructions. Human lung fibroblast (HLuFb) were purchased from Coriell Institute for Medical research (Camden, NJ). *Passages 2–5* cells were used for all experiments and were cultured in DMEM medium containing 15% non-heat-inactivated FBS (Gemini Bioproducts), 1% penicillin/streptomycin, and supplemented with 1× NEAA (Invitrogen).

Immunoblotting. Cells were washed once with cold PBS and resuspended in 100 μl of 1× SDS lysis buffer (62.5 mM Tris·HCl, pH 6.8, 2% wt/vol SDS, 10% glycerol, 50 mM DTT, and 0.01% bromophenol blue). DNA was sheared using an ultrasonicator (Heat Systems-Ultrasonics, Plainview, NY) at 50% output control for 15 s at 4°C. Samples were heated for 5 min at 95°C. Equal amounts of protein (10 μg) for each sample were separated by 10% SDS-PAGE and electroblotted at 20 V for 60 min using a semidry blotting system (BioRad) onto a PVDF membrane. Blots were blocked in 5% BSA in TBS/0.1% Tween 20 (TTBS) for 1 h at ambient temperature before incubating overnight with 1:1,000 dilution of primary antibody in TTBS/0.5% BSA at 4°C. Blots were washed in 3× TTBS for 10 min, for 30 min total. Secondary antibodies (1:1,000 in TTBS) were blotted for 1 h; blots were washed in TBS for at least 2 h before exposing. ECL (Pierce Biotechnology, Rockford, IL) was applied according to the manufacturer's instructions and analyzed on a FujiFilm Image Reader LAS-1000Pro (FujiFilm USA, Valhalla, NY). To normalize for protein loading, blots were stripped using BME Stripping Buffer (10% SDS, β-mercaptoethanol, 0.5 M Tris·HCl) and reblotted for β-actin.

Electrochemiluminescent assays of Met content and activated (phospho-) Met. Met protein content was measured using a two-site electrochemiluminescent immunoassay developed for use with a SectorImager 2400 plate reader (Meso Scale Discovery, Gaithersburg, MD) as described previously (1). Antibodies for capture (BAF-358) and detection (AF-276) were obtained from R&D Systems (Minneapolis, MN). Detection antibodies were tagged with a ruthenium chelate (MSD Sulfo-Tag) per the manufacturer's instructions; in the presence of appropriate redox reagents, the tag emits light when current is applied to the multiwell plate, and this light is measured by the SectorImager CCD camera. Use of a purified recombinant Met ectodomain-Ig fusion protein (358-MT, R&D Systems) as a reference standard permits quantitation as Met mass per mass total extracted cell protein. Met autophosphorylation in cell lysates was measured using the same capture antibody followed by detection with anti-phosphotyrosine antibody 4G10 (Millipore). For time course experiments of Met activation and degradation, cultured cells (184B5 or EA.hy926, respectively) were serum deprived for 48 h and stimulated with HGF or InlB fragments for the indicated time periods. The cells were lysed with ice-cold buffer containing non-ionic detergent, protease, and phosphatase inhibitors; cleared extracts were applied to plates containing immobilized Met capture antibody and with anti-Met, and, in parallel, anti-pY, as described above. All measurements were made on triplicate samples, and results shown are representative of three or more independent experiments. GraphPad Prism 5 software was used for regression analyses and ANOVA.

Neutral comet assay. The neutral comet assay was used to measure double-stranded DNA breaks as an indication of apoptosis as previously described (28). PAEC were either control or treated with Ang II to stimulate apoptosis ± 20 min pretreatment with the $InlB_{36–321}$ monomer, the $InlB_{36–321}$ dimer, or HGF. After 16 h, cells were harvested, counted, and embedded in 1% low-melting point agarose (Sigma) and placed on a comet slide (Trevigen, Gaithersburg, MD). Slides were then placed in lysis solution (2.5 M NaCl, 1% sodium lauryl sarcosinate, 100 mM EDTA, 10 mM Tris base, 0.01% Triton X-100) for 15 min and then washed by immersion in 1× Tris/borate/EDTA buffer (TBE; 0.089 M Tris, 0.089 M boric acid, and 0.002 M EDTA, pH 8.0). The nuclei were subsequently electrophoresed for 10 min at 18 V/cm in 1×TBE. Slides were fixed in 75% ethanol for 10 min and air-dried overnight. Cells were then stained with 1× Sybr Green (Molecular Probes, Eugene, OR). Immediately after staining, comets were visualized with an Olympus FV500 series confocal laser scanning microscope using ×20 magnification at 478-nm excitation and 507-nm emission wavelengths. Between 100 and 150 comets from random fields were scored per experiment and assigned into type A, B, or C categories, based on their tail moments. Type C comets were defined as apoptotic cells as described by Krown et al. 1996 (30).

DNA laddering assay. PAEC were harvested in the medium and pelleted at 1,000 *g*. Pellets were resuspended on ice in lysis buffer (10 mM Tris, 1 mM EDTA, 0.2% Triton, pH 8.0) for 15 min. Cell debris and intact nuclei were removed by centrifugation at 15,000 *g* for 15 min at 4°C. RNA was removed by RNase A (0.06 mg/ml) incubation for 30 min at 37°C. Then, SDS (final concentration at 0.5%) and 0.15 mg/ml of proteinase K were added to the lysate and incubated overnight at 50°C. DNA fragments were precipitated by the addition of 0.1 volume of 5 M NaCl and 1 volume of isopropanol on ice for 10 min. After centrifugation for 15 min at 15,000 *g*, DNA fragments were dissolved in 20 μl of TE buffer. GelPilot DNA Loading Dye (4 μl, Qiagen) was added to this solution and incubated for 10 min at 50°C, and then the DNA was analyzed by 1.5% agarose gel electrophoresis at 20 V for 2 h.

TUNEL assay. PAEC were grown to 80% confluency in 35-mm dishes and treated at indicated time points. TUNEL assay was then performed using Promega DeadEnd Fluorometric TUNEL Assay kit following the manufacturer's protocol.

Cell growth assay. PAEC were seeded at a density of 5×10^4 cells/35 mm dish. To attached cells, HGF, the $InlB_{36–321}$ monomer, or the $InlB_{36–321}$ dimer was added in triplicate wells to the medium on *days 1*, *2*, *4*, *6*, and *8*. Cells were trypsinized and counted in triplicate using a hemacytometer at the indicated time points.

Migration assay. PAEC were trypsinized, washed, and plated at a density of 3×10^5 cells/well in 12-well/plate Transwell (Corning, Corning, NY) dishes (12-μm pore size). Cells were allowed to attach for 3 h and were then treated in both upper and lower chambers with HGF, the $InlB_{36–321}$ monomer, or the $InlB_{36–321}$ dimer in triplicate wells. After 16 h, cells migrated through the Transwell insert were fixed for 15 min in 100% methanol and stained for 1 h in 0.94% crystal violet (Fisher, Fairlawn, NJ) in 20% methanol. The insert was rinsed in a large volume of H_2O, and the upper side of the membrane was cleaned using a cotton swab. Remaining migrated cells were counted by microscopy.

Animals and ex vivo cultures. All treatment of animals was performed according to National Institutes of Health, Department of Defense, and with institutional IACUC approval. Sprague-Dawley rats (Taconic, Germantown, NY) were housed, 1 female with litter per cage, in a facility accredited by the Association for Assessment and Accreditation of Laboratory Animal Care International. Animal rooms were maintained at 21 ± 2°C, 50% ± 10% humidity, and 12-h light/dark cycle. Commercial rodent ration (Harlan Teklad Rodent Diet 8604) and water were freely available. Rat pups were obtained on postnatal *days 10–11*. Animals were anesthetized with pentobarbital and decapitated or euthanized with Fatal-Plus. The surface of the anterior chest wall and upper abdomen were sterilized with 70% ethanol. After the trachea was exposed, a small nick was made to insert a 22-gauge needle with a short piece of polyethelene tube attached. Two lines were tied around the trachea to stabilize and to prevent the tube from slipping out. Through a midline abdominal

incision, the chest cavity was exposed, and the animal was exsanguinated by dissecting the abdominal aorta. The right ventricle was punctured, and the lungs were perfused with sterile PBS to remove the blood. Using aseptic technique, the trachea, lungs, and the heart were dissected from the animal. To obtain lung slices for the ex vivo culture, the lungs were inflated with 1% low-melting point agarose dissolved in RPMI medium. Agarose was instilled as a liquid into the trachea using a syringe and to fully inflate the lungs. The lungs were placed in sterile cell culture plates and at 4°C for at least 30 min to solidify the agarose. The heart was then excised from the lung, and each lobe of the lungs was embedded in 1% agarose. The agarose-filled and embedded lungs were then chopped on a McIlwain tissue chopper (GeneQ Quebec, Canada) into 500-μm-thick slices. The lung explant slices were incubated in RPMI 1640 containing 10% FBS, 1% penicillin/streptomycin, and 0.5% fungizone for 1 h at 37°C in a humidified chamber with 5% CO_2. Lung slices were then transferred to the wells of a 24-well cell culture plate with treatments performed in triplicate for 16 h.

Statistical analysis. Means ± SD were calculated, and statistically significant differences between two groups were determined by the Student's *t*-test. For three or more groups, statistical analysis was performed using one-way ANOVA, followed by Bonferroni postanalysis, as appropriate; $P < 0.05$ was considered statistically significant. Statistical software for all analysis was SigmaStat 3.1 (Point Richmond, CA).

RESULTS

Differential signal transduction by the 1×InlB$_{36–321}$ and the 2×InlB$_{36–321}$. The fragment of the InlB protein from amino acids 36 to 321 was previously demonstrated to bind and partially activate the Met receptor in transformed mammalian cells (48). We cloned this portion of the InlB protein with a 6-His tag for purification as a monomer (1×InlB$_{36–321}$) and as a tandem repeat with a linker peptide (2×InlB$_{36–321}$). The proteins were expressed in *E. coli*, purified on a Ni-NTA column, and treated for the removal of endotoxin. The purified InlB$_{36–321}$ monomer resulted in a protein of 32 kDa, whereas the purified 2×InlB$_{36–321}$ resulted in a 65-kDa protein (Supplementary Data, Fig. S1. Supplemental Material for this article is available online at the Journal website).

We confirmed that the purified recombinant proteins activated the Met receptor kinase using a human mammary epithelial cell line, 184B5, which has relatively high Met protein levels, and with serum deprivation, displays very low basal Met kinase activity and robust activation by HGF (7, 12). We determined in 184B5 cells that the EC_{50} concentrations for Met activation are 0.25 nM, 1.0 nM, and 5.0 nM for HGF, 2×lnlB$_{36–321}$, and 1×lnlB$_{36–321}$, respectively (data not shown). For time course experiments, ligands were used at concentrations determined to provide maximal receptor activation. The time courses of Met activation were determined using nonlinear regression analysis and have R^2 values of 0.9413, 0.9363, and 0.9277 for HGF, 1×InlB$_{36–321}$, and 2×InlB$_{36–321}$, respectively (Fig. 1*A*). A two-way ANOVA shows that the InlB 1× and 2× curves are significantly different (20.04% total variance; $P < 0.0001$). Although 2×InlB$_{36–321}$ reaches an initial maximum that is higher than that observed for HGF, it was used at sixfold greater molar concentration. Two-way ANOVA of these curves yields a 14.07% variance overall ($P < 0.0001$). The analysis suggests that the rates of Met activation by HGF and 2×InlB$_{36–321}$ are similar, whereas that for 1×InlB$_{36–321}$ is slower by comparison. All three ligands achieved a similar sustained level of Met activation after 60 min. These results confirm Met binding and activation by both InlB$_{36–321}$ proteins and are consistent with a prior report of increased potency associated with dimeric form of InlB$_{36–321}$ (8).

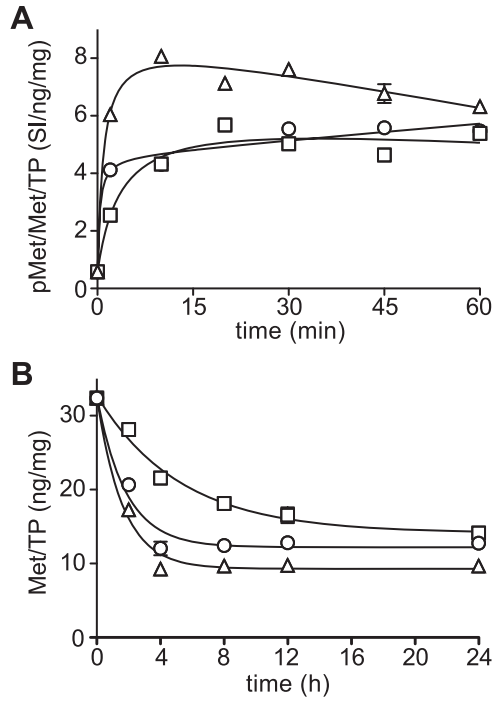

Fig. 1. Temporal profiles of ligand-stimulated Met activation and degradation. *A*: Met activation, expressed as phosphoMet signal intensity units normalized to Met protein and total cellular protein (SI/ng/mg), in 184B5 normal human epithelial cells stimulated with HGF (circles), 1×InlB$_{36–321}$ (squares), or 2×InlB$_{36–321}$ (triangles). Ligands were used at concentrations determined to provide maximal receptor activation at 20 min: 1.0 nM, 12.5 nM, and 6.1 nM for HGF, 1×InlB$_{36–321}$, and 2×InlB$_{36–321}$, respectively. Significant differences among the curves were determined using 2-way ANOVA and are discussed in the text. *B*: Met degradation, expressed as Met normalized to total protein (ng/mg) in EA.hy926 human hybrid vascular endothelial cells stimulated with HGF (circles), 1×InlB$_{36–321}$ (squares), or 2×InlB$_{36–321}$ (triangles). Ligands were used at concentrations listed in *A*. Significant differences among the curves were determined using 2-way ANOVA and are discussed in the text.

Met degradation experiments were performed using the human hybrid vascular endothelial cell line EA.hy926. This cell line was selected for analysis of Met degradation because it has a relatively low level of Met protein, and ligand-driven changes in receptor abundance are readily measured. The time courses of Met protein content change in response to ligand stimulation are shown in Fig. 1*B*. Concentrations of ligands are the same as in Fig. 1*A*. The curves were determined using nonlinear regression analysis and have R^2 values of 0.9693, 0.9809, and 0.9842 for HGF, 1×InlB$_{36–321}$, and 2×InlB$_{36–321}$, respectively. Similar to the Met activation profiles, the results show that the rates of Met degradation driven by HGF and 2×InlB$_{36–321}$ are similar, whereas that for 1×InlB$_{36–321}$ is slower by comparison. The initial difference in HGF and 2× InlB$_{36–321}$ degradation maxima is less than that observed in activation experiments, consistent with the slower rate of change overall and the greater complexity of degradation compared with Met activation. Although all three ligands reduce Met content significantly after 24 h, a two-way ANOVA shows that the 1×InlB$_{36–321}$ and 2×InlB$_{36–321}$ curves are significantly different (18.4% total variance; $P <$

0.0001). Similar analysis of the HGF and 2×$InlB_{36–321}$ curves reveals 2.44% total variance between the curves, which, while statistically significant, yields only a 10% difference in Met abundance from 8 to 24 h; the HGF and 1×$InlB_{36–321}$ curves have a fourfold higher total variance of 9.92% ($P < 0.0001$), but ultimately converge after 24 h.

Each of the purified $InlB_{36–321}$ proteins was used to treat primary PAEC to compare signal transduction pathway activation in nontransformed, non-immortalized cells. We compared activation of ERK1/2 MAPK, Akt, and STAT3 by HGF and the two InlB constructs, as these three pathways have been implicated in HGF-induced proliferation (10, 44). We previously determined that maximal ERK1/2 activation occurred within 5–30 min by HGF and the InlB constructs in PAEC (35). Western blots showed that within 15 min, phospho-ERK1/2 increased by threefold and fivefold following exposure to 1.2 or 2.5 nM HGF, respectively (Fig. 2*A*). Treatment with 0.3, 1.0, or 5.0 nM 2×$InlB_{36–321}$ resulted in twofold, twofold, and fourfold increases in phospho-ERK, respectively. In contrast, treatment with 0.3 nM 1×$InlB_{36–321}$ had no significant effect on ERK activation. Treatment with 1.0 and 5.0 nM 1×$InlB_{36–321}$ induced twofold and fourfold increases in ERK activation, similar to the level of activation by 2×$InlB_{36–321}$.

The PI3K/Akt pathway has been shown to be required for cellular proliferation by HGF (12). Akt activation is associated with its phosphorylation. Within 15 min of treatment with HGF, an approximately twofold increase in phospho-Akt was observed (Fig. 2*B*). Treatment with 0.6 nM 2×$InlB_{36–321}$ resulted in a 50% increase in phospho-Akt within 15 min and a twofold increase at 30 min. Treatment with 6.0 nM 2×$InlB_{36–321}$ provided a 2-fold and 2.4-fold increase in phospho-Akt at 15 and 30 min, respectively. Activation of Akt by 10 nM 1×$InlB_{36–321}$ was not detected at any time point (Fig. 2*B*), even though this concentration of 1×$InlB_{36–321}$ was sufficient to induce ERK1/2 phosphorylation.

STAT3 activation by HGF has been shown to participate in cellular proliferation in tissue repair (44). HGF induced a ~12-fold increase in phosphorylation within 15 min (Fig. 2*C*). Treatment with 2×$InlB_{36–321}$ for 30 min (both 0.6 and 6 nM) induced similar levels of STAT3 phosphorylation as HGF. However, although 1×$InlB_{36–321}$ significantly activated STAT3, maximal levels were only fivefold above control levels. Together, these results suggest that 0.6 nM 2×$InlB_{36–321}$ induced significant phosphorylation of all three Met signaling molecules, ERK1/2, Akt, and STAT3, at levels similar to HGF. In contrast, the 1×$InlB_{36–321}$ activates Met, but subsequent signaling is weaker than that of 2×$InlB_{36–321}$.

Cell motility and cell survival by 2×$InlB_{36–321}$ compared with 1×$InlB_{36–321}$. Cell motility is an important activity induced by HGF through Met activation. Previous reports demonstrated that $InlB_{36–321}$ induced migration in transformed cell types (48). We compared motility in PAEC induced by both the 1×$InlB_{36–321}$ and 2×$InlB_{36–321}$. Levels of migration in control cultures were 60 ± 5 (Fig. 3). HGF induced significant increase of motility (123 ± 7, $P < 0.05$). The 2×$InlB_{36–321}$ induced cell migration equivalent to that induced by full-length HGF (133 ± 10), which was significantly higher than migration induced by the 1×$InlB_{36–321}$ (89 ± 14; $P < 0.05$ compared with 2×$InlB_{36–321}$; Fig. 3).

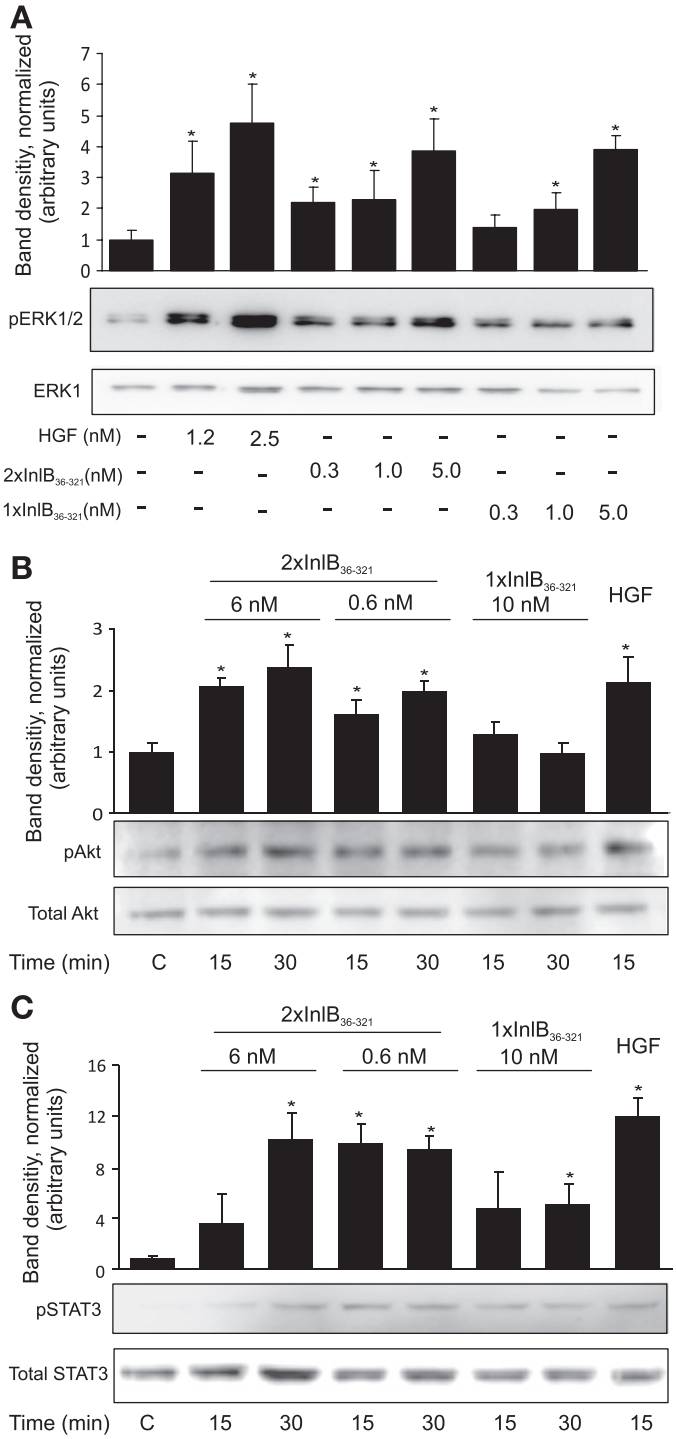

Fig. 2. Activation of ERK1/2, Akt, and STAT3 by 1× and 2×$InlB_{36–321}$ and HGF in primary lung endothelial cells. Pulmonary artery endothelial cells (PAEC) were grown to 80% confluence and placed in 0.01% FBS overnight before treatment. *A*: cells were treated with the indicated concentrations of HGF, 1×$InlB_{36–321}$, and 2×$InlB_{36–321}$ for 15 min at the indicated concentrations. Cell lysates were blotted for phosphorylated ERK1/2 (pERK1/2). Blots were stripped and reprobed for total ERK1. *B* and *C*: cells were treated with the indicated concentrations of 1×$InlB_{36–321}$ [0.4 μg/ml (10^{-8} M)] and 2×$InlB_{36–321}$ [0.4 μg/ml (6 ×10^{-9} M) and 0.04 μg/ml (6 ×10^{-10} M), respectively] for the indicated times. HGF (25 ng/ml, 0.3 ×10^{-9} M) was used as control. Lysates were blotted either for phosphorylated Akt (pAkt) (*B*) or phosphorylated STAT3 (pSTAT) (*C*). Blots were stripped and probed for total Akt or total STAT3. Representative blots are shown. Bar graphs show the means ± SD from 3 experiments. *$P < 0.05$ from control.

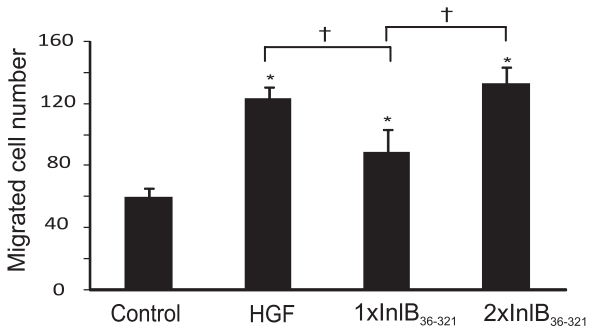

Fig. 3. Comparison of cellular motility induced by 1×and 2×InlB$_{36-321}$ and HGF in primary lung endothelial cells. PAEC were plated at a density of 3 ×10^5 cells in triplicate in wells of a Transwell dish. Cells were placed in 0.01% FBS with either no addition, 1×InlB$_{36-321}$ (4.2 μg/ml, 1.2 ×10^{-7} M), 2×InlB$_{36-321}$ (0.4 μg/ml, 6 ×10^{-9} M), or HGF (25 ng/ml, 3 ×10^{-10} M). After 16 h, cells were fixed and stained, and the numbers of cells migrating through the membrane were determined. Data show averages ± SD; *$P < 0.05$ from basal migration levels. †$P < 0.05$ from InlB monomer-induced migration levels. Experiments were repeated at least 3 times, and representative data are shown.

Our laboratory recently demonstrated that Ang II, a profibrotic peptide, activates intrinsic apoptosis (34), and bleomycin, a chemotherapeutic agent that induces lung fibrosis in humans and animal models, activates the extrinsic pathway of apoptosis in PAEC (43). We examined the cell survival activity of both 1×and 2×InlB$_{36-321}$. HGF reduced apoptosis to 11% ± 0.9, $P < 0.05$, compared with Ang II alone, and 2×InlB$_{36-321}$ (6.0 and 0.6 nM) provided protection at a similar level with HGF as determined by the Neutral Comet assay (Fig. 4*A*). Both HGF and 2×InlB$_{36-321}$ also provided similar levels of cell survival (~5% apoptosis, $P < 0.05$) as determined by the TUNEL assay (Fig. 4*B*). Pretreatment of cells for 1 h with 10 nM 1×InlB$_{36-321}$ also resulted in significant protection of PAEC from Ang II-induced DNA fragmentation as determined by Comet assay, but to a lesser extent compared with the other ligands (32% ± 0.4, $P < 0.05$ from Ang II alone). However, TUNEL assay showed that treatment with 10 nM 1×InlB$_{36-321}$ provided levels of cell survival similar to that of the other ligands (Fig. 4*B*). The addition of HGF or either InlB$_{36-321}$ peptide alone did not statistically alter the apoptosis from basal levels in either assay. Together, these data suggest that 1×InlB$_{36-321}$ and 2×InlB$_{36-321}$ provide similar levels of anti-apoptotic activity.

To confirm the anti-apoptotic activity of 2×InlB$_{36-321}$, we conducted apoptosis-specific DNA laddering assays. Treatment of PAEC with Ang II or bleomycin resulted in DNA laddering within 16 h (Fig. 4*C*). Treatment of cells with 2×InlB$_{36-321}$ for 20 min before apoptosis stimulation completely prevented DNA laddering induced by both Ang II and bleomycin. Together, these data demonstrate that the InlB$_{36-321}$ proteins, like HGF, promote cell survival from Ang II.

The 2×InlB$_{36-321}$ induces proliferation in primary lung endothelial cells. Because the InlB dimer activates PI3K/Akt and STAT3 in addition to ERK1/2, three signaling pathways that are involved in proliferation by Met (12), we examined cell growth in primary endothelial cells. In agreement with findings by others (47), we found that 1×InlB$_{36-321}$ failed to induce proliferation in PAEC (Fig. 5). However, 2×InlB$_{36-321}$ induced proliferation equivalent to that induced by HGF (Fig. 5). Together with the prior results, these findings suggest that in PAEC, activating the ERK1/2 cascade without activating the PI3K/Akt axis is sufficient for a motogenic but not mitogenic response to Met activation.

The 2×InlB$_{36-321}$ activates cell survival in ex vivo lung tissue. A number of studies have utilized ex vivo lung cultures as substitutes for in vivo models. This technique has the

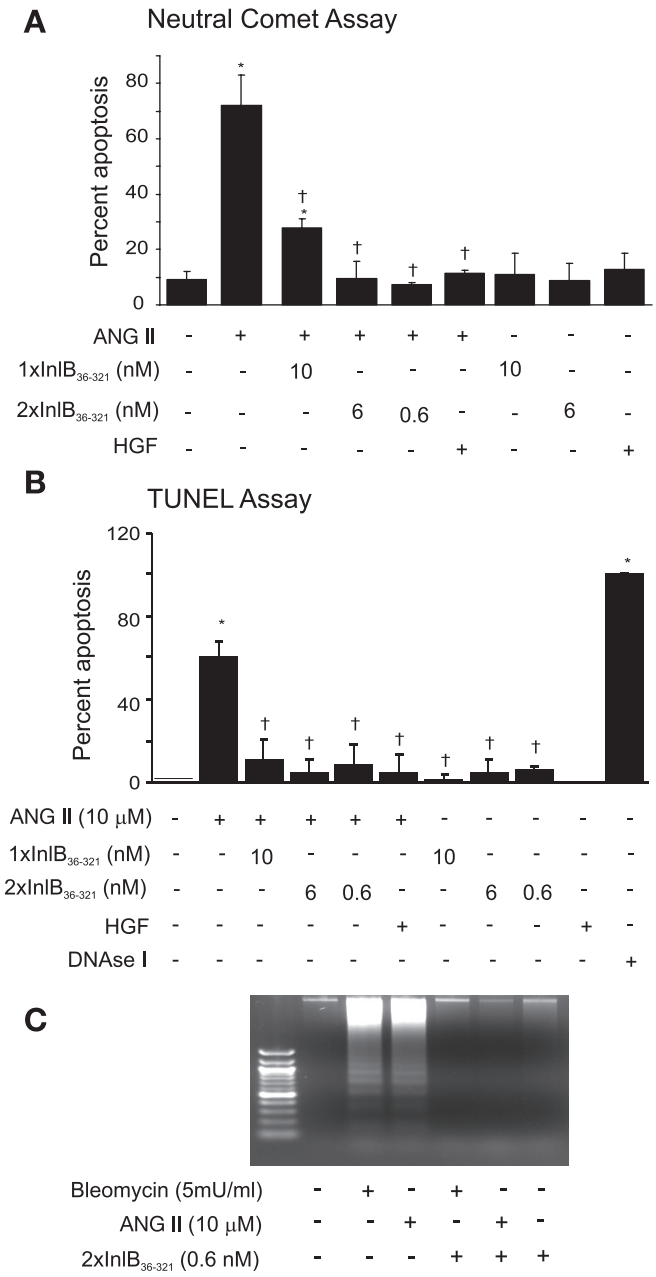

Fig. 4. Comparison of activation of cellular survival by 1×and 2×InlB$_{36-321}$ and HGF in primary lung endothelial cells. PAEC were grown to 80% confluence and placed in 0.01% FBS. Cells were treated either with 1×InlB$_{36-321}$ (10^{-8} M), 2×InlB$_{36-321}$ (6 ×10^{-9} or 6 ×10^{-10} M), or HGF (3 × 10^{-10} M), for 1 h before the addition of Ang II (10 μM). *A*: after 16 h, DNA fragmentation was analyzed by Neutral Comet assays. *B*: evaluation of apoptotic cells by TUNEL assay. Data show means ± SD, $n = 3$; *$P < 0.05$ from control, †$P < 0.05$ from Ang II-treated cells. A positive control for DNA degradation utilized treatment with DNase I (1.4 U/ml). *C*: cells were exposed to 2×InlB$_{36-321}$ or HGF for 1 h before Ang II or bleomycin treatment. After 16 h, DNA laddering was analyzed by agarose gel electrophoresis. The experiment was performed at least 3 times, and representative data are shown.

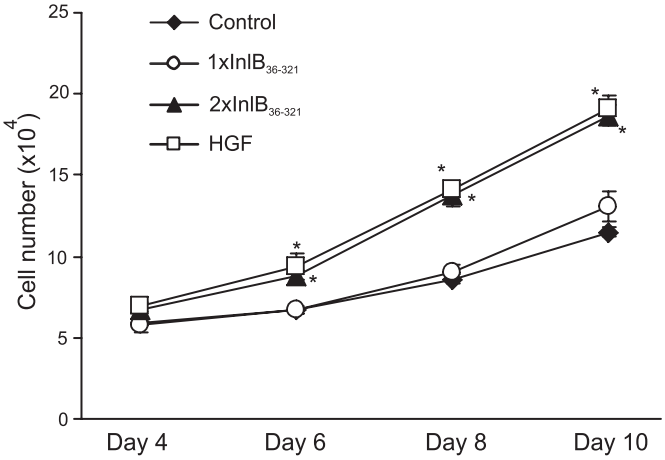

Fig. 5. Comparison of proliferative activity of the 1×and 2×$InlB_{36–321}$, and HGF in primary lung endothelial cells. PAEC were plated at a density of 5 ×10^4 cells/35-mm dish in triplicate and allowed to attach for 6 h. The cells were placed in 1% FBS with either no addition (control), 1×$InlB_{36–321}$ (4.2 μg/ml, 1.2 ×10^{-7} M), 2×$InlB_{36–321}$ (0.4 μg/ml, 6 ×10^{-9} M), or HGF (25 ng/ml, 3 ×10^{-10} M). Media with additions was replaced on *days 1*, *2*, and *4*. Cells were counted on *days 4*, *6*, *8*, and *10*. Data show means ± SD. *$P < 0.05$ from basal levels, $n = 3$.

advantage of allowing lung-specific assessments from potentially confounding whole body effects (21). Because an isolated organ experiment sustains the architecture and functionality of the tissue, it represents a closer model to in vivo than the in vitro models from a single cell type. Studies have shown that alveolar cells spontaneously divide and correctly differentiate in ex vivo lung slice cultures (26), and this technique has been used to determine drug responses, apoptosis, and cell survival (18, 32, 36). The ex vivo lung model has been demonstrated to act as a reliable model for in vivo studies to demonstrate the role of Ang II signaling in lung cell apoptosis from profibrotic stimuli (36, 38). To determine whether the $InlB_{36–321}$ can protect cells in lung from Ang II-induced apoptosis, we examined caspase 3 activation in rat ex vivo lung slices cultured in the presence or absence of HGF, 1×, or 2×$InlB_{36–321}$. Caspase 3 was activated by the addition of Ang II within 16 h as shown by Western blot using specific antibodies (Fig. 6). HGF and both $InlB_{36–321}$ peptides suppressed caspase 3 activation significantly to near baseline levels. Compared with 1×$InlB_{36–321}$, 2×$InlB_{36–321}$ was able to inhibit caspase 3 activation at 10-fold lower concentration (Fig. 6). None of the ligands activated caspase 3 when applied in the absence of Ang II.

Activation of ERK1/2 by $InlB_{36–321}$ is cell type specific. Our results suggested that the $InlB_{36–321}$ peptides activate HGF receptor Met and its downstream signaling, and we wanted to verify that the activity of the $InlB_{36–321}$ was Met-specific. Met is predominantly expressed in cells from epithelial origin, whereas expression of HGF was usually restricted to cells of mesenchymal origin (53). Therefore, we used Met-negative fibroblast cells to evaluate the specificity of ERK1/2 activation in response to both $InlB_{36–321}$ peptides and HGF. As expected, both 1×$InlB_{36–321}$ and 2×$InlB_{36–321}$ activated ERK1/2, similarly to HGF, within 15 min of treatment in PAEC (Fig. 7*A*), but not in primary fibroblast cultures that do not express Met (Fig. 7*B*). As a positive control, we show that EGF activates ERK1/2 in primary fibroblast cultures (Fig. 7).

DISCUSSION

Here we show that a fragment of the *L. monocytogenes* InlB, amino acids 36–321 (1×$InlB_{36–321}$), activates the ERK1/2 and STAT3 pathways in primary lung endothelial cells, resulting in motility, as well as cell survival from Ang II-induced apoptosis. Expression of the $InlB_{36–321}$ as a modified tandem repeat (2×$InlB_{36–321}$) results in the activation of an additional pathway, the PI3K/Akt pathway. Cell growth and cell migration assays showed improved activity of 2×$InlB_{36–321}$ compared with the 1×form. We propose that this additional signal transduction pathway is correlated with improved motility compared with 1×$InlB_{36–321}$, as well as with the added biological activity of cell proliferation in PAEC cultures. Our results using ex vivo lung slices represent an alternative to in vivo methods in measuring cellular signaling mechanisms. Therefore, our findings of protection from Ang II-induced apoptosis in our lung slice cultures by 1×$InlB_{36–321}$ may be considered predictive for the activity of this protein in vivo.

HGF signaling through the Met receptor induces normal tissue repair in a manner that restores tissue structure and prevents the development of extensive scar formation or fibrosis in liver, kidney, heart, brain, and lung (27, 40, 41, 46, 59, 66, 67). The importance of HGF in tissue repair and the cost and difficulty associated with producing recombinant, active HGF protein has prompted researchers to seek alternative means to activate the pathway, such as inducing endogenous *HGF* gene expression and protein production using natural and synthetic compounds (45, 51, 60) or using exogenous expression methods. However, HGF has been shown to be an important factor in the progression of tumorigenesis, discouraging the treatment of human patients with HGF in retroviral systems that would induce its permanent or constitutive expression. Instead, transient, nonviral in vivo gene transfer techniques have been investigated and demonstrated to be effective in a

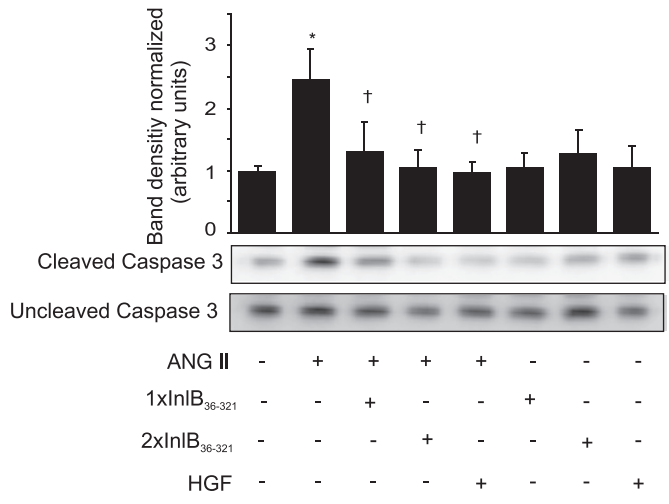

Fig. 6. Cell survival activity of 1×, 2×$InlB_{36–321}$, and HGF in lung tissue explants. Ex vivo lung tissue slices were prepared from rat lungs. Tissue was placed in medium with 10% FBS, incubated for 16 h, and treated with 1×$InlB_{36–321}$ (10^{-8} M), 2×$InlB_{36–321}$ (6 ×10^{-10} M), or HGF (3 ×10^{-10} M) for 1 h before Ang II (10 μM) exposure; after 16 h, whole lysates were prepared for activated caspase 3 Western blotting. Blots were stripped and reprobed for uncleaved caspase 3 and analyzed by band densitometry. Data show means ± SD from 3 independent experiments. *$P < 0.05$ from basal levels. Representative blots are shown. †$P < 0.05$ from AngII-treated cells.

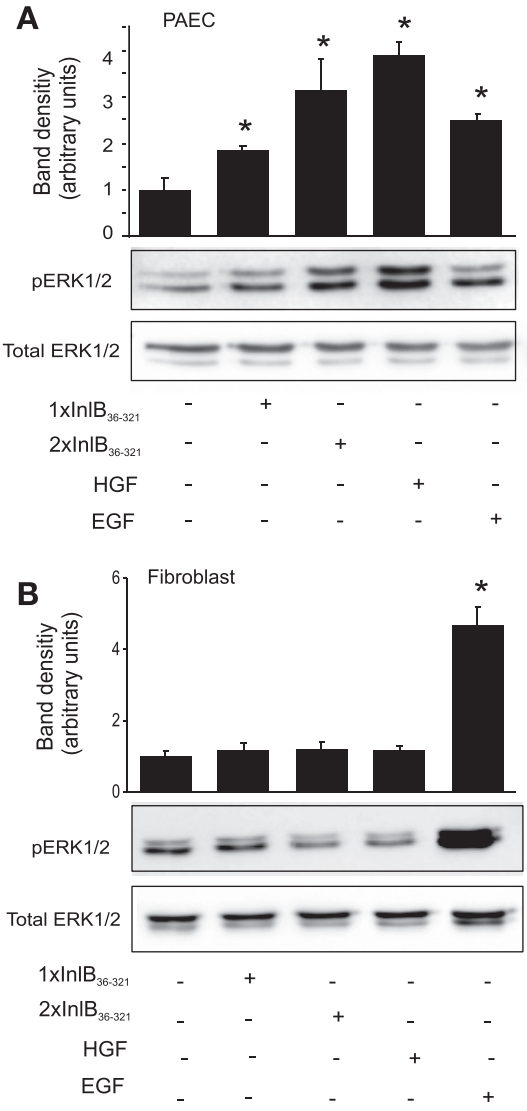

Fig. 7. Evaluation of ERK1/2 activation in pulmonary endothelial cells vs. fibroblasts. Cells were grown to 80% confluence and placed overnight in starving media containing 0.01% FBS. They were then treated with $1\times(10^{-8}$ M), $2\times InlB_{36-321}$ (6×10^{-10} M), or HGF (3×10^{-10} M) for 15 min. Cell lysates were used for Western blot with anti-phospho-ERK1/2. Blots were stripped and reblotted for total ERK for normalization. EGF (100 ng/ml) was used as control. *A*: ERK1/2 activation in PAEC. *B*: ERK1/2 activation in primary human lung fibroblast cell culture. Bar graphs show the means ± SD from 3 independent experiments. $*P < 0.05$ from control. Representative blots are shown.

variety of animal models of organ fibrosis (11, 19, 51, 56, 65, 67). These methods are currently being tested in early clinical trials for HGF exogenous expression (42).

Studies suggest that the ERK1/2, PI3K/Akt, and the STAT3 pathways are required for the mitogenic activity of HGF (10). HGF-stimulated mitogenesis seems to depend on duration of ERK1/2 activation in some cell types (12). In others, both ERK1/2 and STAT3 activation are needed for cell proliferation (44). Our data using the InlB peptides suggest that ERK1/2 and STAT3 activation are not sufficient for mitogenesis in PAEC downstream of Met activation and that the PI3K/Akt pathway is also required.

We propose that the novel $2\times InlB_{36-321}$ may have therapeutic potential similar to that of full-length HGF. Additionally, treatment using $2\times InlB_{36-321}$ has potential advantages over the use of HGF protein for wound repair. One complication for the use of HGF protein is that HGF must be activated by cleavage at R494 by an extracellular protease on the target cell (53). This additional requirement for processing of HGF to its active form has implications for the use of a cytokine or other agent to stimulate HGF production, since stimulation of HGF production doesn't ensure that it will be active in the vicinity of the target cell. In contrast, the $2\times InlB_{36-321}$ is synthesized in its active form. A second complication of the use of HGF is that HGF is a potent factor in cancer progression (13). In contrast, a recent report indicates that InlB protein binding to Met downregulates the receptor on the surface of cancer cells (16), and it has been proposed that InlB and its fragments may be useful for suppression of Met signaling in cancer (9). Our cell culture studies of Met downregulation suggest that HGF and $2\times InlB_{36-321}$ are similar, whereas that for $1\times InlB_{36-321}$ is slower by comparison.

It is widely viewed that tyrosine kinase receptors are activated by dimerization, but that multiple mechanisms have evolved to induce the active dimeric state (55). For the Met receptor, dimers have been observed of truncated versions of the receptor with ligands in crystal structures (15, 17). Cell culture data has indicated that Met clustering does occur in cells during Met activation (14), but discrete dimers of full-length Met have not yet been demonstrated in intact cells. A recent study by Ferraris et al. (15) described signaling and biological activities in cancer cells of an InlB dimer that was engineered using a disulfide bond centered on the convex face of the LRR helix, allowing the formation of an antiparallel arrangement of two $InlB_{36-321}$ fragments. This construct differs significantly from the construct used in the present work, which provides a head-to-tail arrangement of the $InlB_{36-321}$ fragments. The structural differences between the two InlB constructs have significant implications for the physical mechanism of Met receptor activation, which has eluded full characterization for two decades by virtue of its complexity. Our findings together with those of Ferraris et al. suggest that both the antiparallel dimer and tandemly repeated $InlB_{36-321}$ fragment are sufficient to induce Met dimerization and/or clustering. A better understanding of the mechanism of Met receptor activation may facilitate the improvement of both inhibitors and agonists for this important signaling pathway.

ACKNOWLEDGMENTS

We thank Dr. Suzanne B. Bausch and W. Brad Rittase (USUHS, Bethesda, MD) for supplying rat lung tissue and for help in development of the ex vivo slice culture technique. We also thank Dr. Laurel Lenz for his gift of genomic DNA from *Listeria*.

GRANTS

This work was supported by National Institutes of Health Grant HL-073929, a USUHS research grant, a joint USUHS-Henry Jackson Foundation Technology Development Award to R. M. Day, and by an American Heart Association predoctoral fellowship to Y. H. Lee. This research was also supported in part by the Intramural Research Program of the NIH, National Cancer Institute, Center for Cancer Research.

DISCLOSURES

R. M. Day, O. Mungunsukh, and Y. H. Lee have filed a patent in the United States Patent and Trademark Office for the use of a modified InlB protein: Tissue Repair, Prevention, and Treatment of Fibrosis Using a Chimeric *L. monocytogenes* InlB Protein (Provisional patent No. 61/122,055). Some of the

REFERENCES

1. **Athauda G, Giubellino A, Coleman JA, Horak C, Steeg PS, Lee MJ, Trepel J, Wimberly J, Sun J, Coxon A, Burgess TL, Bottaro DP.** c-Met ectodomain shedding rate correlates with malignant potential. *Clin Cancer Res* 12: 4154–4162, 2006.
2. **Banerjee M, Copp J, Vuga D, Marino M, Chapman T, van der Geer P, Ghosh P.** GW domains of the *Listeria monocytogenes* invasion protein InlB are required for potentiation of Met activation. *Mol Microbiol* 52: 257–271, 2004.
3. **Bierne H, Cossart P.** InlB, a surface protein of *Listeria monocytogenes* that behaves as an invasin and a growth factor. *J Cell Sci* 115: 3357–3367, 2002.
4. **Birchmeier C, Gherardi E.** Developmental roles of HGF/SF and its receptor, the c-Met tyrosine kinase. *Trends Cell Biol* 8: 404–410, 1998.
5. **Bogatkevich GS, Ludwicka-Bradley A, Highland KB, Hant F, Nietert PJ, Singleton CB, Feghali-Bostwick CA, Silver RM.** Impairment of the antifibrotic effect of hepatocyte growth factor in lung fibroblasts from African Americans: possible role in systemic sclerosis. *Arthritis Rheum* 56: 2432–2442, 2007.
6. **Bosse T, Ehinger J, Czuchra A, Benesch S, Steffen A, Wu X, Schloen K, Niemann HH, Scita G, Stradal TE, Brakebusch C, Rottner K.** Cdc42 and phosphoinositide 3-kinase drive Rac-mediated actin polymerization downstream of c-Met in distinct and common pathways. *Mol Cell Biol* 27: 6615–6628, 2007.
7. **Chan AM, Rubin JS, Bottaro DP, Hirschfield DW, Chedid M, Aaronson SA.** Identification of a competitive HGF antagonist encoded by an alternative transcript. *Science* 254: 1382–1385, 1991.
8. **Cioce V, Csaky KG, Chan AM, Bottaro DP, Taylor WG, Jensen R, Aaronson SA, Rubin JS.** Hepatocyte growth factor (HGF)/NK1 is a naturally occurring HGF/scatter factor variant with partial agonist/antagonist activity. *J Biol Chem* 271: 13110–13115, 1996.
9. **Cossart P, Veiga E.** Compositions for the treatment of tumor pathologies, comprising internalin B (LN1B) of Listeria monocytogenes protein or a fragment thereof. U. S. Patent 11,372,462. Filed March 10, 2006.
10. **Crosby LM, Waters CM.** Epithelial repair mechanisms in the lung. *Am J Physiol Lung Cell Mol Physiol* 298: L715–L731, 2010.
11. **Cruzado JM, Lloberas N, Torras J, Riera M, Fillat C, Herrero-Fresneda I, Aran JM, Alperovich G, Vidal A, Grinyo JM.** Regression of advanced diabetic nephropathy by hepatocyte growth factor gene therapy in rats. *Diabetes* 53: 1119–1127, 2004.
12. **Day RM, Cioce V, Breckenridge D, Castagnino P, Bottaro DP.** Differential signaling by alternative HGF isoforms through c-Met: activation of both MAP kinase and PI 3-kinase pathways is insufficient for mitogenesis. *Oncogene* 18: 3399–3406, 1999.
13. **Eder JP, Vande Woude GF, Boerner SA, LoRusso PM.** Novel therapeutic inhibitors of the c-Met signaling pathway in cancer. *Clin Cancer Res* 15: 2207–2214, 2009.
14. **Faletto DL, Tsarfaty I, Kmiecik TE, Gonzatti M, Suzuki T, Vande Woude GF.** Evidence for non-covalent clusters of the c-met proto-oncogene product. *Oncogene* 7: 1149–1157, 1992.
15. **Ferraris DM, Gherardi E, Di Y, Heinz DW, Niemann HH.** Ligand-mediated dimerization of the met receptor tyrosine kinase by the bacterial invasion protein InlB. *J Mol Biol* 395: 522–532, 2010.
16. **Gao X, Lorinczi M, Hill KS, Brooks NC, Dokainish H, Ireton K, Elferink LA.** Met receptor tyrosine kinase degradation is altered in response to the leucine-rich repeat of the *Listeria* invasion protein internalin B. *J Biol Chem* 284: 774–783, 2009.
17. **Gherardi E, Sandin S, Petoukhov MV, Finch J, Youles ME, Ofverstedt LG, Miguel RN, Blundell TL, Vande Woude GF, Skoglund U, Svergun DI.** Structural basis of hepatocyte growth factor/scatter factor and MET signalling. *Proc Natl Acad Sci USA* 103: 4046–4051, 2006.
18. **Hackett TL, Holloway R, Holgate ST, Warner JA.** Dynamics of pro-inflammatory and anti-inflammatory cytokine release during acute inflammation in chronic obstructive pulmonary disease: an ex vivo study. *Respir Res* 9: 47, 2008.
19. **Hayashi K, Nakamura S, Morishita R, Moriguchi A, Aoki M, Matsumoto K, Nakamura T, Kaneda Y, Sakai N, Ogihara T.** In vivo transfer of human hepatocyte growth factor gene accelerates re-endothelialization and inhibits neointimal formation after balloon injury in rat model. *Gene Ther* 7: 1664–1671, 2000.
20. **Hegab AE, Kubo H, Yamaya M, Asada M, He M, Fujino N, Mizuno S, Nakamura T.** Intranasal HGF administration ameliorates the physiologic and morphologic changes in lung emphysema. *Mol Ther* 16: 1417–1426, 2008.
21. **Henjakovic M, Martin C, Hoymann HG, Sewald K, Ressmeyer AR, Dassow C, Pohlmann G, Krug N, Uhlig S, Braun A.** Ex vivo lung function measurements in precision-cut lung slices (PCLS) from chemical allergen-sensitized mice represent a suitable alternative to in vivo studies. *Toxicol Sci* 106: 444–453, 2008.
22. **Huh CG, Factor VM, Sanchez A, Uchida K, Conner EA, Thorgeirsson SS.** Hepatocyte growth factor/c-met signaling pathway is required for efficient liver regeneration and repair. *Proc Natl Acad Sci USA* 101: 4477–4482, 2004.
23. **Hummers LK, Hall A, Wigley FM, Simons M.** Abnormalities in the regulators of angiogenesis in patients with scleroderma. *J Rheumatol* 36: 576–582, 2009.
24. **Ireton K, Payrastre B, Chap H, Ogawa W, Sakaue H, Kasuga M, Cossart P.** A role for phosphoinositide 3-kinase in bacterial invasion. *Science* 274: 780–782, 1996.
25. **Kamimoto M, Mizuno S, Matsumoto K, Nakamura T.** Hepatocyte growth factor prevents multiple organ injuries in endotoxemic mice through a heme oxygenase-1-dependent mechanism. *Biochem Biophys Res Commun* 380: 333–337, 2009.
26. **Kinnard WV, Tuder R, Papst P, Fisher JH.** Regulation of alveolar type II cell differentiation and proliferation in adult rat lung explants. *Am J Respir Cell Mol Biol* 11: 416–425, 1994.
27. **Kitamura K, Iwanami A, Nakamura M, Yamane J, Watanabe K, Suzuki Y, Miyazawa D, Shibata S, Funakoshi H, Miyatake S, Coffin RS, Nakamura T, Toyama Y, Okano H.** Hepatocyte growth factor promotes endogenous repair and functional recovery after spinal cord injury. *J Neurosci Res* 85: 2332–2342, 2007.
28. **Kitta K, Day RM, Ikeda T, Suzuki YJ.** Hepatocyte growth factor protects cardiac myocytes against oxidative stress-induced apoptosis. *Free Radic Biol Med* 31: 902–910, 2001.
29. **Kondo I, Ohmori K, Oshita A, Takeuchi H, Fuke S, Shinomiya K, Noma T, Namba T, Kohno M.** Treatment of acute myocardial infarction by hepatocyte growth factor gene transfer: the first demonstration of myocardial transfer of a "functional" gene using ultrasonic microbubble destruction. *J Am Coll Cardiol* 44: 644–653, 2004.
30. **Krown KA, Page MT, Nguyen C, Zechner D, Gutierrez V, Comstock KL, Glembotski CG, Quintana PJE, Sabbadini RA.** Tumor necrosis factor alpha-induced apoptosis in cardiac myocytes: involvement of the sphingolipid signaling cascade in cardiac cell death. *J Clin Invest* 98: 2854–2865, 1996.
31. **Kuroiwa T, Kakishita E, Hamano T, Kataoka Y, Seto Y, Iwata N, Kaneda Y, Matsumoto K, Nakamura T, Ueki T, Fujimoto J, Iwasaki T.** Hepatocyte growth factor ameliorates acute graft-versus-host disease and promotes hematopoietic function. *J Clin Invest* 107: 1365–1373, 2001.
32. **Lang DS, Droemann D, Schultz H, Branscheid D, Martin C, Ressmeyer AR, Zabel P, Vollmer E, Goldmann T.** A novel human ex vivo model for the analysis of molecular events during lung cancer chemotherapy. *Respir Res* 8: 43, 2007.
33. **Lassus P, Heikkila P, Andersson LC, von Boguslawski K, Andersson S.** Lower concentration of pulmonary hepatocyte growth factor is associated with more severe lung disease in preterm infants. *J Pediatr* 143: 199–202, 2003.
34. **Lee YH, Mungunsukh O, Tutino RL, Marquez AP, Day RM.** Angiotensin-II-induced apoptosis requires regulation of nucleolin and Bcl-x_L by SHP-2 in primary lung endothelial cells. *J Cell Sci* 123: 1634–1643, 2010.
35. **Lee YH, Suzuki YJ, Griffin AJ, Day RM.** Hepatocyte growth factor regulates cyclooxygenase-2 expression via beta-catenin, Akt, and p42/p44 MAPK in human bronchial epithelial cells. *Am J Physiol Lung Cell Mol Physiol* 294: L778–L793, 2008.
36. **Li X, Rayford H, Uhal BD.** Essential roles for angiotensin receptor AT1a in bleomycin-induced apoptosis and lung fibrosis in mice. *Am J Pathol* 163: 2523–2530, 2003.

37. **Maina F, Hilton MC, Ponzetto C, Davies AM, Klein R.** Met receptor signaling is required for sensory nerve development and HGF promotes axonal growth and survival of sensory neurons. *Genes Dev* 11: 3341–3350, 1997.
38. **Mancini GB, Khalil N.** Angiotensin II type 1 receptor blocker inhibits pulmonary injury. *Clin Invest Med* 28: 118–126, 2005.
39. **Marchand-Adam S, Marchal J, Cohen M, Soler P, Gerard B, Castier Y, Leseche G, Valeyre D, Mal H, Aubier M, Dehoux M, Crestani B.** Defect of hepatocyte growth factor secretion by fibroblasts in idiopathic pulmonary fibrosis. *Am J Respir Crit Care Med* 168: 1156–1161, 2003.
40. **Matsumoto K, Nakamura T.** HGF: its organotrophic role and therapeutic potential. *Ciba Symp* 212: 198–211; discussion 211–194, 1997.
41. **Mizuno S, Matsumoto K, Nakamura T.** Hepatocyte growth factor suppresses interstitial fibrosis in a mouse model of obstructive nephropathy. *Kidney Int* 59: 1304–1314, 2001.
42. **Morishita R, Aoki M, Hashiya N, Makino H, Yamasaki K, Azuma J, Sawa Y, Matsuda H, Kaneda Y, Ogihara T.** Safety evaluation of clinical gene therapy using hepatocyte growth factor to treat peripheral arterial disease. *Hypertension* 44: 203–209, 2004.
43. **Mungunsukh O, Griffin AJ, Lee YH, Day RM.** Bleomycin induces the extrinsic apoptotic pathway in pulmonary endothelial cells. *Am J Physiol Lung Cell Mol Physiol* 298: L696–L703, 2010.
44. **Nakagami H, Morishita R, Yamamoto K, Taniyama Y, Aoki M, Matsumoto K, Nakamura T, Kaneda Y, Horiuchi M, Ogihara T.** Mitogenic and antiapoptotic actions of hepatocyte growth factor through ERK, STAT3, and AKT in endothelial cells. *Hypertension* 37: 581–586, 2001.
45. **Nakamura K, Sata M, Iwata H, Sakai Y, Hirata Y, Kugiyama K, Nagai R.** A synthetic small molecule, ONO-1301, enhances endogenous growth factor expression and augments angiogenesis in the ischaemic heart. *Clin Sci* 112: 607–616, 2007.
46. **Nakamura T, Mizuno S, Matsumoto K, Sawa Y, Matsuda H, Nakamura T.** Myocardial protection from ischemia/reperfusion injury by endogenous and exogenous HGF. *J Clin Invest* 106: 1511–1519, 2000.
47. **Niemann HH, Jager V, Butler PJ, van den Heuvel J, Schmidt S, Ferraris D, Gherardi E, Heinz DW.** Structure of the human receptor tyrosine kinase met in complex with the *Listeria* invasion protein InlB. *Cell* 130: 235–246, 2007.
48. **Niemann HH, Petoukhov MV, Hartlein M, Moulin M, Gherardi E, Timmins P, Heinz DW, Svergun DI.** X-ray and neutron small-angle scattering analysis of the complex formed by the Met receptor and the *Listeria monocytogenes* invasion protein InlB. *J Mol Biol* 377: 489–500, 2008.
49. **Ohmichi H, Matsumoto K, Nakamura T.** In vivo mitogenic action of HGF on lung epithelial cells: pulmotrophic role in lung regeneration. *Am J Physiol Lung Cell Mol Physiol* 270: L1031–L1039, 1996.
50. **Okunishi K, Sasaki O, Okasora T, Nakagome K, Imamura M, Harada H, Matsumoto T, Tanaka R, Yamamoto K, Tabata Y, Dohi M.** Intratracheal delivery of hepatocyte growth factor directly attenuates allergic airway inflammation in mice. *Int Arch Allergy Immunol* 149, *Suppl* 1: 14–20, 2009.
51. **Ono M, Sawa Y, Matsumoto K, Nakamura T, Kaneda Y, Matsuda H.** In vivo gene transfection with hepatocyte growth factor via the pulmonary artery induces angiogenesis in the rat lung. *Circulation* 106: I264–I269, 2002.
52. **Ponzetto C, Pante G, Prunotto C, Ieraci A, Maina F.** Met signaling mutants as tools for developmental studies. *Int J Dev Biol* 44: 645–653, 2000.
53. **Rubin JS, Bottaro DP, Aaronson SA.** Hepatocyte growth factor/scatter factor and its receptor, the c-met proto-oncogene product. *Biochim Biophys Acta* 1155: 357–371, 1993.
54. **Santos OF, Barros EJ, Yang XM, Matsumoto K, Nakamura T, Park M, Nigam SK.** Involvement of hepatocyte growth factor in kidney development. *Dev Biol* 163: 525–529, 1994.
55. **Schlessinger J.** Cell signaling by receptor tyrosine kinases. *Cell* 103: 211–225, 2000.
56. **Shigemura N, Sawa Y, Mizuno S, Ono M, Ohta M, Nakamura T, Kaneda Y, Matsuda H.** Amelioration of pulmonary emphysema by in vivo gene transfection with hepatocyte growth factor in rats. *Circulation* 111: 1407–1414, 2005.
57. **Shimamura M, Sato N, Waguri S, Uchiyama Y, Hayashi T, Iida H, Nakamura T, Ogihara T, Kaneda Y, Morishita R.** Gene transfer of hepatocyte growth factor gene improves learning and memory in the chronic stage of cerebral infarction. *Hypertension* 47: 742–751, 2006.
58. **Stahl SJ, Wingfield PT, Kaufman JD, Pannell LK, Cioce V, Sakata H, Taylor WG, Rubin JS, Bottaro DP.** Functional and biophysical characterization of recombinant human hepatocyte growth factor isoforms produced in *Escherichia coli*. *Biochem J* 326: 763–772, 1997.
59. **Tahara M, Matsumoto K, Nukiwa T, Nakamura T.** Hepatocyte growth factor leads to recovery from alcohol-induced fatty liver in rats. *J Clin Invest* 103: 313–320, 1999.
60. **Takahashi M, Hata Y, Terano A.** Effect of sofalcone on the expression of hepatocyte growth factor (HGF) and a brief review of HGF in the stomach. *J Clin Gastroenterol* 25, *Suppl* 1: S21–S27, 1997.
61. **Ueki T, Kaneda Y, Tsutsui H, Nakanishi K, Sawa Y, Morishita R, Matsumoto K, Nakamura T, Takahashi H, Okamoto E, Fujimoto J.** Hepatocyte growth factor gene therapy of liver cirrhosis in rats. *Nature Med* 5: 226–230, 1999.
62. **Umeda Y, Marui T, Matsuno Y, Shirahashi K, Iwata H, Takagi H, Matsumoto K, Nakamura T, Kosugi A, Mori Y, Takemura H.** Skeletal muscle targeting in vivo electroporation-mediated HGF gene therapy of bleomycin-induced pulmonary fibrosis in mice. *Lab Invest* 84: 836–844, 2004.
63. **Veiga E, Cossart P.** Listeria InlB takes a different route to Met. *Cell* 130: 218–219, 2007.
64. **Vila MR, Nakamura T, Real FX.** Hepatocyte growth factor is a potent mitogen for normal human pancreas cells in vitro. *Lab Invest* 73: 409–418, 1995.
65. **Watanabe M, Ebina M, Orson FM, Nakamura A, Kubota K, Koinuma D, Akiyama K, Maemondo M, Okouchi S, Tahara M, Matsumoto K, Nakamura T, Nukiwa T.** Hepatocyte growth factor gene transfer to alveolar septa for effective suppression of lung fibrosis. *Mol Ther* 12: 58–67, 2005.
66. **Yaekashiwa M, Nakayama S, Ohnuma K, Sakai T, Abe T, Satoh K, Matsumoto K, Nakamura T, Takahashi T, Nukiwa T.** Simultaneous or delayed administration of hepatocyte growth factor equally represses the fibrotic changes in murine lung injury induced by bleomycin. A morphologic study. *Am J Respir Crit Care Med* 156: 1937–1944, 1997.
67. **Yoshimura S, Morishita R, Hayashi K, Kokuzawa J, Aoki M, Matsumoto K, Nakamura T, Ogihara T, Sakai N, Kaneda Y.** Gene transfer of hepatocyte growth factor to subarachnoid space in cerebral hypoperfusion model. *Hypertension* 39: 1028–1034, 2002.